

SPINELS AND OXYGEN FUGACITY IN OLIVINE-PHYRIC AND LHERZOLITIC SHERGOTTITES.

¹C.A. Goodrich, ²C.D.K. Herd and ³L.A. Taylor. ¹Hawaii Institute of Geophysics and Planetology, University of Hawaii at Manoa, Honolulu, HI 96822, USA (cyrena @higp.hawaii.edu). ²Lunar and Planetary Institute, 3600 Bay Area Blvd, Houston, TX 77058, USA. ³Planetary Geosciences Institute, University of Tennessee, Knoxville, TN 37966, USA.

Introduction: Amongst martian meteorites correlations between La/Yb values and initial Sr and Nd isotopic compositions indicate the presence of long-term incompatible element-enriched and -depleted reservoirs, and suggest that martian magmatism is characterized by mixing between these reservoirs [1-4]. Recent work [5] has suggested that oxygen fugacity (fO_2) is also correlated with these parameters, implying that the reservoirs are oxidized and reduced, respectively. Oxygen fugacity estimates have been based on coexisting Fe-Ti oxides (ulvöspinel-ilmenite) for 5 basaltic shergottites and the groundmasses of olivine-phyric [6] shergottites EETA79001 lithology A (EET-A) and Dhofar 019 [7,8]. Oxygen fugacity was also estimated for olivine-phyric shergottite DaG 476 using coexisting olivine-pyroxene-chromite assemblages [5], which may reflect magmatic conditions more accurately than late-crystallizing Fe-Ti oxides. We extend this approach to olivine-phyric shergottites SaU 005, EET-A, Dhofar 019 and NWA 1110 (possibly paired with NWA 1068 [9,10]), and to lherzolitic shergottite ALHA77005.

Spinels in Olivine-Phyric Shergottites: Spinels in SaU 005 and EET-A are described by [11,12]. Spinels in Dhofar 019 (see also [8]) and NWA 1110 have similar characteristics. In all these shergottites, low-Ti chromite occurs as individual grains included in olivine (type 1), and in composite grains (type 2) as cores rimmed by ulvöspinel (Fig. 1) included in the more ferroan olivine and in the groundmass. Ulvöspinel also occurs as individual grains included in the more ferroan olivine and in the groundmass. Chromites (both type 1 and cores of type 2 grains) are normally zoned with small ranges of Cr# (SaU 005: 0.81-0.79; EET-A: 0.84-0.80; Dhofar 019: 0.82-0.80; NWA 1110: 0.86-0.84). Their magnetite contents recalculated from electron microprobe analyses are ~1-3% in SaU 005 and Dhofar 019, 2-4% in EET-A, and ~4-11% in NWA 1110 (Fig. 2). Fe#s show variations indicating subsolidus reequilibration with surrounding olivine or groundmass.

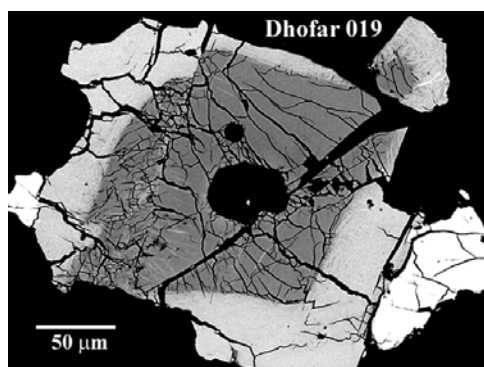


Fig. 1. Type 2 spinels in olivine-phyric shergottites show a distinct core-rim structure. Cores are low-Ti chromite and rims are ulvöspinel, with a gap in Ti content (Fig. 2).

Type 2 spinels show a gap in Ti content (largest in EET-A, smallest in NWA 1110) between cores and rims (Fig. 2), as observed in some lunar and terrestrial spinels [13-15]. In Dhofar 019 and SaU 005 magnetite contents of rims are similar to those of chromite cores, whereas in EET-A, they are significantly higher (with a gap); in NWA 1110, there is a continuous and dramatic increase in magnetite content from core through rims (Fig. 2).

Spinels in Lherzolitic Shergottites: Spinels in the groundmass of ALHA77005 (and LEW 88516) have no core/rim structure, and show complete solid solution between chromite and ulvöspinel (Fig. 2b). They have high Cr# (~0.87), and magnetite contents similar to the earliest chromites in NWA 1110 (Fig. 2b). Spinels included in olivine have not yet been examined in detail.

Olivine-Pyroxene-Spinel Assemblages: Early olivine-pyroxene-chromite assemblages were identified, where possible, from spatial relations (chromite + pyroxene included in olivine), and otherwise, by assuming that the chromites with the highest Cr# (earliest crystallizing) and the lowest Fe# (least reequilibrated) co-crystallized with the most magnesian olivine (Fo 81 in EET-A; Fo 74 in SaU 005 and ALHA77005; Fo 73 in Dhofar 019 and NWA 1110) and equilibrium low-Ca pyroxene ($KD_{Fe/Mg}$ (ol/lpyx) ~1.2). In addition, assemblages representing the onset of ulvöspinel crystallization were identified from occurrences of type 2 spinels in olivine (Fo ≤60 in EET-A, ≤68 in SaU 005, ≤64 in Dhofar 019 and ≤62 in NWA 1110). Oxygen fugacities were calculated for all assemblages as in [5].

Results: Results for the early assemblages are ($T \pm 40^\circ C / fO_2 \pm 0.5$ relative to QFM): Dhofar 019 – (1099/-3.7), similar to the estimate of [8] from Fe-Ti oxides; SaU 005 – (1017/-3.8); EET-A – (921/-2.8); NWA 1110 – (1024/-1.7). Results for the later assemblages are: Dhofar 019 – (967/-2.8); SaU 005 – (1039/-3.4); EET-A – (925/-1.8), consistent with the estimate of [7] for Fe-Ti oxides in the groundmass; NWA 1110 – (836/-0.5). Results for spinels in the groundmass of ALHA77005 were highly variable and will be investigated further.

Discussion: For early crystallization conditions, estimated fO_2 increases from SaU 005/Dhofar 019 to EET-A to NWA 1110 (consistent with the calculated magnetite contents of the chromites). Relatively oxidizing conditions for NWA 1110 may be reflected in the small Ti gap shown by its type 2 spinels. Hill and Roeder [16] found experimentally that this compositional gap, which is due to loss of spinel (early chromite) as a stable phase followed by its later reappearance as titanomagnetite/ulvöspinel, occurred only at low fO_2 (below ~QFM at magmatic temperatures, although for shergottitic compositions this limit may be different than for the terrestrial basalts used in that study). On the other hand, our results suggest that fO_2 is not the only factor that affects the presence/size of the gap. For example, the large gap in EET-A may result from mixing of an early, reduced magma with a more oxidized magma (following the

interpretation of [11,12] that early chromites are xenolithic relative to the magma from which the ulvöspinel crystallized). Cooling rate and reequilibration may also affect the size of the gap. Results for type 1 chromites in ALHA77005 (in which the gap is completely absent) might clarify the degree to which the chromite-ulvöspinel gap can be used as an indication of oxygen fugacity.

Figure 3 shows La/Yb vs. fO_2 for shergottites, with results from this work and [5,7]. NWA 1110 has fO_2 within error of previous determinations for Shergotty, Zagami and Los Angeles (LA), and if it is paired with NWA 1068 [9,10] it should have La/Yb similar to these basaltic shergottites as well; however, this is not yet known. The proper La/Yb value for the early chromite assemblage in EET-A (Ex) is uncertain. In the interpretation of [11,12], this assemblage is xenolithic relative to most of the rest of the rock. REE data of [17] for melt inclusions in this chromite show significantly lower La/Yb than bulk EET-A, suggesting that the xenoliths may have been derived from a more depleted reservoir than the magma from which the bulk of the rock crystallized; however, those data should be considered preliminary. Furthermore, there are uncertainties in the interpretation of EA (groundmass of EET-A or appearance of ulvöspinel) and EB (lithology B of EETA79001). If xenolithic models for EET-A [11,12,18,19] are correct, then EA may represent early conditions for an assimilating magma. However, it may simply represent a later stage of crystallization of Ex. Likewise, in some models [11,12] EB is thought to be a late fractionate of Ex or EA, rather than a magma composition. Considering all these uncertainties, La/Yb vs. fO_2 relations among shergottites (Fig. 3) may indicate two groups – a reduced, LREE-depleted group and a more oxidized and enriched group – rather than a correlation curve as previously suggested [5].

References: [1] Shih C.-Y. et al. (1982) *GCA* **46**, 2323. [2] Jones J.H. (1989) *Proc. Lunar Planet. Sci. Conf.* **19**, 465; (2002) *LPI Contribution No. 1134*, 27. [3] Borg L.E. et al. (1987) *GCA* **61**, 4915; Borg L.E. (2002) *LPI Contribution No. 1134*, 9. [4] McSween H.Y., Jr. (2002) *MAPS* **37**, 7. [5] Herd C.D.K. et al. (2002) *GCA* **66**, 2025; Herd C.D.K. (2002) *LPI Contribution No. 1134*, 21. [6] Goodrich C.A. (2002) *MAPS* **37**, B31. [7] Herd C.D.K. et al. (2002) *Am. Min.* **86**, 1015. [8] Taylor L.A. et al. (2002) *MAPS* **37**, 1107. [9] Goodrich C.A. et al. (2003) *this volume*. [10] Barrat J.A. et al. (2002) *GCA* **66**, 3505. [11] Goodrich C.A. (2003) *GCA*, in press. [12] Goodrich C.A. (2002) *LPI Contribution No. 1134*, 17. [13] Taylor L.A. et al. (1971) *Proc. Lunar Sci. Conf.* **2nd**, 855. [14] Haggerty S.E. (1976) in *Oxide Minerals. Min. Soc. America Short Course Notes* **3**. [15] El Goresy et al. (1976) *Proc. Lunar Sci. Conf.* **7th**, 1261. [16] Hill R. and Roeder P. (1974) *J. Geology* **82**, 709. [17] Zipfel J. and Goodrich C.A. (2002) *LPS* **33**, #1279. [18] McSween H.Y., Jr. and Jarosewich E. (1983) *GCA* **47**, 1501. [19] Steele I.M. and Smith J.V. (1982) *Proc. 13th Lunar Planet. Sci. Conf.*, *JGR* **87**, A375.

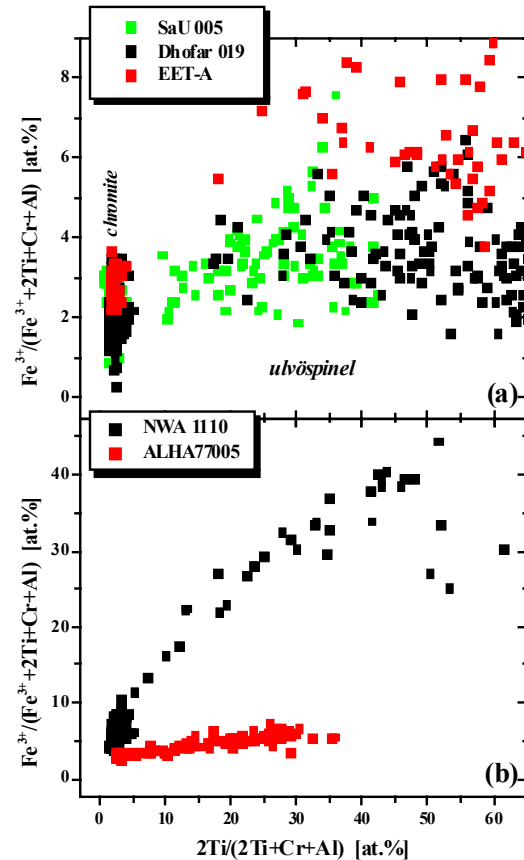


Fig. 2. Ulvöspinel vs. magnetite component for spinels in olivine-phyric and ilherzolitic shergottites. Chromites include type 1 and cores of type 2 grains. Spinels in the groundmass of ALHA77005 show continuous chromite-ulvöspinel solid solution and no core-rim structure.

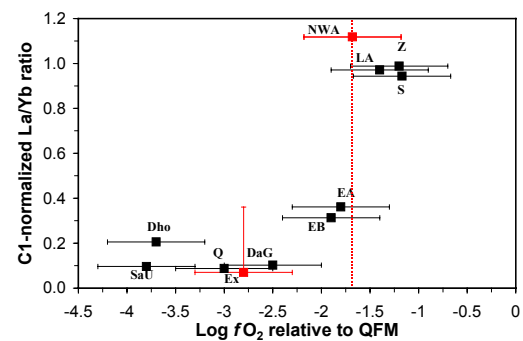


Fig. 3. La/Yb vs. fO_2 estimated in this work and [5,7] for shergottites. Dho = Dhofar 019; SaU = SaU 005; Q = QUE94201; DaG = DaG 476; Ex = early chromite assemblage in EET-A (this work); EA = groundmass of EET-A (this work and [7]); EB = EET-B; Z = Zagami; S = Shergotty; LA = Los Angeles; NWA = NWA 1110 (La/Yb plotted is for NWA 1068). See text for discussion.